Tectonophysics 478 (2009) 111–118

Contents lists available at ScienceDirect

Tectonophysics

journal homepage: www.elsevier.com/locate/tecto

Simple models for the Beattie Magnetic Anomaly in South Africa

Yoann Quesnel [a,*], Ute Weckmann [a,b], Oliver Ritter [a], Jacek Stankiewicz [a], Vincent Lesur [a], Mioara Mandea [a], Benoit Langlais [c,d], Christophe Sotin [e], Armand Galdéano [f]

[a] Helmholtz Centre Potsdam GFZ German Research Centre for Geosciences, Telegrafenberg, 14473 Potsdam, Germany
[b] University of Potsdam, Institute for Geosciences, Karl-Liebknecht-Strasse 24, 14476 Potsdam, Germany
[c] Université de Nantes, Laboratoire de Planétologie et Géodynamique de Nantes, 2, rue de la Houssinière, 44322 Nantes, France
[d] CNRS UMR 6112, 2, rue de la Houssinière, 44322 Nantes, France
[e] Jet Propulsion Laboratory, 4800 Oak Grove Drive, Pasadena, California 91109, USA
[f] Institut de Physique du Globe de Paris, CNRS, UMR 7154, Géomagnétisme, 4, place Jussieu, 75252 Paris cedex 05, France

ARTICLE INFO

Article history:
Received 30 November 2007
Received in revised form 13 October 2008
Accepted 25 November 2008
Available online 6 December 2008

Keywords:
Beattie Magnetic Anomaly
Crust
Magnetization
Forward modeling
Inversion
Magnetotelluric and seismic experiments

ABSTRACT

The origin of the approximately 1000 km-long Beattie Magnetic Anomaly (BMA) in South Africa remains unclear and contentious. Key issues include the width, depth and magnetization of its source. In this study, we use uniformly magnetized spheres, prisms and cylinders to provide the simplest possible models which predict the 1 km-altitude aeromagnetic measurements along a profile across the BMA. The source parameters are adjusted by forward modeling. In case of a sphere, an inversion technique is applied to refine the parameters. Our results suggest that two similarly magnetized and adjacent sources, with a vertical offset, can explain the observed magnetic anomaly. The best fitting model corresponds to two highly-magnetized (>5 A m^{-1}) sheet-like prisms, extending from 9 to 12 km depth, and from 13 to 18 km depth, respectively, and with a total width reaching 80 km. Other less-preferred models show thicker and deeper magnetized volumes. Associated magnetizations seem to be mostly induced, although a weak remanent component is required to improve the fit. We also compare our results with the interpretation of independent magnetotelluric and seismic experiments along the same profile. It suggests that the geological sources for the BMA are mostly located in the middle crust and may be displaced by a shear zone or a fault. Contrary to previous models suggesting a serpentinized sliver of paleo-oceanic crust within the Natal–Namaqua Mobile Belt, we propose that granulite-facies mid-crustal rocks within this belt may cause the BMA.

1. Introduction

The Beattie Magnetic Anomaly (BMA) extends for almost 1000 km in E–W direction over the southern part of Southern Africa (Fig. 1). It spatially correlates with the Southern Cape Conductive Belt (SCCB), a 100–200 km wide, deep electrical conductivity anomaly (de Beer et al., 1982).

The origin of both these continental-scale geophysical features remains unclear. In particular, the hypothesis that the same geological sources may account for both anomalies is debated. For instance, de Beer et al. (1982) suggested serpentinized rocks, relics of an ancient oceanic lithosphere, as the sources for the BMA and SCCB. According to Pitts et al. (1992) and Harvey et al. (2001), these serpentinites may represent the southern boundary of the Proterozoic granitoid rocks of the Namaqua–Natal Mobile Belt (see Fig. 1). Other authors invoked mineralized thrusts (Corner, 1989), as well as shear zones (Thomas et al., 1992) as potential sources for the anomalies. Several-km thick sediments of the Karoo Basin (South African Committee on Stratigraphy, 1980) conceal the bedrock in this region, which implies that these contrasting ideas can only be tested from a geophysical perspective.

Recently, Weckmann et al. (2007a,b) showed new results of two magnetotelluric (MT) profiles across the BMA and the SCCB (Fig. 1). They find a narrow conductive zone below the center of the BMA, inclined either southward beneath the western profile or northward in the eastern profile. Weckmann et al. (2007b) argue in favor of a conductive shear zone that cuts a broad magnetic source. Stankiewicz et al. (2007) presented the results of two seismic refraction surveys, whereas Lindeque et al. (2007) showed those of a seismic reflection experiment. The seismic reflection line and part of the western seismic refraction line follow the western MT profile, where we focus our magnetic study (Fig. 1). Both these recent seismic surveys identified a mid-crustal seismic (velocity or reflectivity) anomaly zone that could potentially represent the source of the BMA.

In our study, we use uniformly magnetized bodies to investigate the possible source of the BMA by fitting the aeromagnetic anomaly profile that follows the MT and western seismic lines. Our aim is to find the simplest one- or two-body model in order to estimate how

* Corresponding author. Present address: CEREGE, Europôle Méditerranéen de l'Arbois, BP 80, 13545 Aix-en-Provence Cedex 04, France. Tel.: +33 442971536; fax: +33 442971590.
E-mail addresses: quesnel@cerege.fr (Y. Quesnel), uweck@gfz-potsdam.de (U. Weckmann), oritter@gfz-potsdam.de (O. Ritter), jacek@gfz-potsdam.de (J. Stankiewicz), lesur@gfz-potsdam.de (V. Lesur), mioara@gfz-potsdam.de (M. Mandea), benoit.langlais@univ-nantes.fr (B. Langlais), christophe.sotin@jpl.nasa.gov (C. Sotin), galdeano@ipgp.jussieu.fr (A. Galdéano).

0040-1951/$ – see front matter © 2008 Elsevier B.V. All rights reserved.
doi:10.1016/j.tecto.2008.11.027

wide, deep and magnetized the source of the BMA is in this area. We also compare our simple magnetic modeling results with recent MT and seismic interpretations to re-address the controversially discussed geological origin for the BMA.

2. Geological context

Major geological features of South Africa are the Archean Kaapvaal Craton in the Northeast, the Mesoproterozoic Namaqua Natal Mobile Belt from West to East, the Paleozoic Cape Fold Belt in the West and South, and the Paleozoic–Mesozoic sedimentary Karoo Basin (Fig. 1), which is composed of the Karoo and Cape Supergroup (de Wit and Ransome, 1992). The Karoo Basin covers more than the half of South Africa, reaching 5–6 km of maximum thickness (Cloetingh et al., 1992).

Here, we investigate the area where the western MT and seismic refraction experiments, as well as the seismic reflection experiment, were recently conducted by the GFZ German Research Centre for Geosciences of Potsdam (Lindeque et al., 2007; Stankiewicz et al., 2007; Weckmann et al., 2007a,b). Fig. 2 presents the location of the studied magnetic profile over a geological map of this area between 21 and 23°E, −31.3 and −33.3°N (Vorster, 2003). It shows that the outcrops along this profile mostly correspond to the thin shales of the Beaufort Group, which is part of the Karoo sedimentary sequence. Jurassic dolerite sills and dikes intrude the Karoo sediments north of the Great Escarpment, a watershed. The southern termination of the profile reaches the sedimentary formations of the Dwyka and Ecca Groups, and ends at the transition to the Cape Supergroup rocks. The detailed stratigraphy of the Karoo Basin near this profile has been revealed by boreholes (Cloetingh et al., 1992). Below the Karoo Basin, a granitic basement belonging to the Mesoproterozoic Namaqua–Natal Mobile Belt has been revealed, but no further information about the possible sources of the BMA are available.

3. Magnetic dataset

The aeromagnetic dataset over South Africa (Fig. 1) allows to analyze the BMA. These data correspond to the *SANABOZI.txt* file provided by the Southern African Development Community (http://www.sadc.int), and used to generate the first Magnetic Anomaly Map of the World (Korhonen et al., 2007). This dataset was compiled using several initial subsets derived from aeromagnetic surveys flown in the early 1980s over the southern part of Africa at different altitudes, and upward or downward continued to a mean altitude of 1 km. Processing of the initial data (removal of the reference field, diurnal variation correction, leveling and filtering) was originally done for each subset independently. We are not able to check the quality of this processing, since these original raw measurements are not available. Fig. 1 shows the magnetic anomaly map with data upward continued to a 5 km level (altitude used for the first Magnetic Anomaly Map of the World). The most prominent magnetic anomaly corresponds to the BMA in South Africa. It is a broad magnetic anomaly, with a width ranging from 100 km to a minimum value of 10 km, and extending for approximately 1000 km in an E–W direction (Fig. 1). In its western part, the BMA splits into two branches, but both of them seem to end over the western section of the Cape Fold Belt region. Along the eastern part of the BMA, the eastern strike direction changes to a northeastern strike direction before reaching the Indian Ocean. Some comparable anomaly chains are observed in South America and Antarctica, at locations that surrounded South Africa prior to Gondwana break-up (Corner, 1989; Corner and

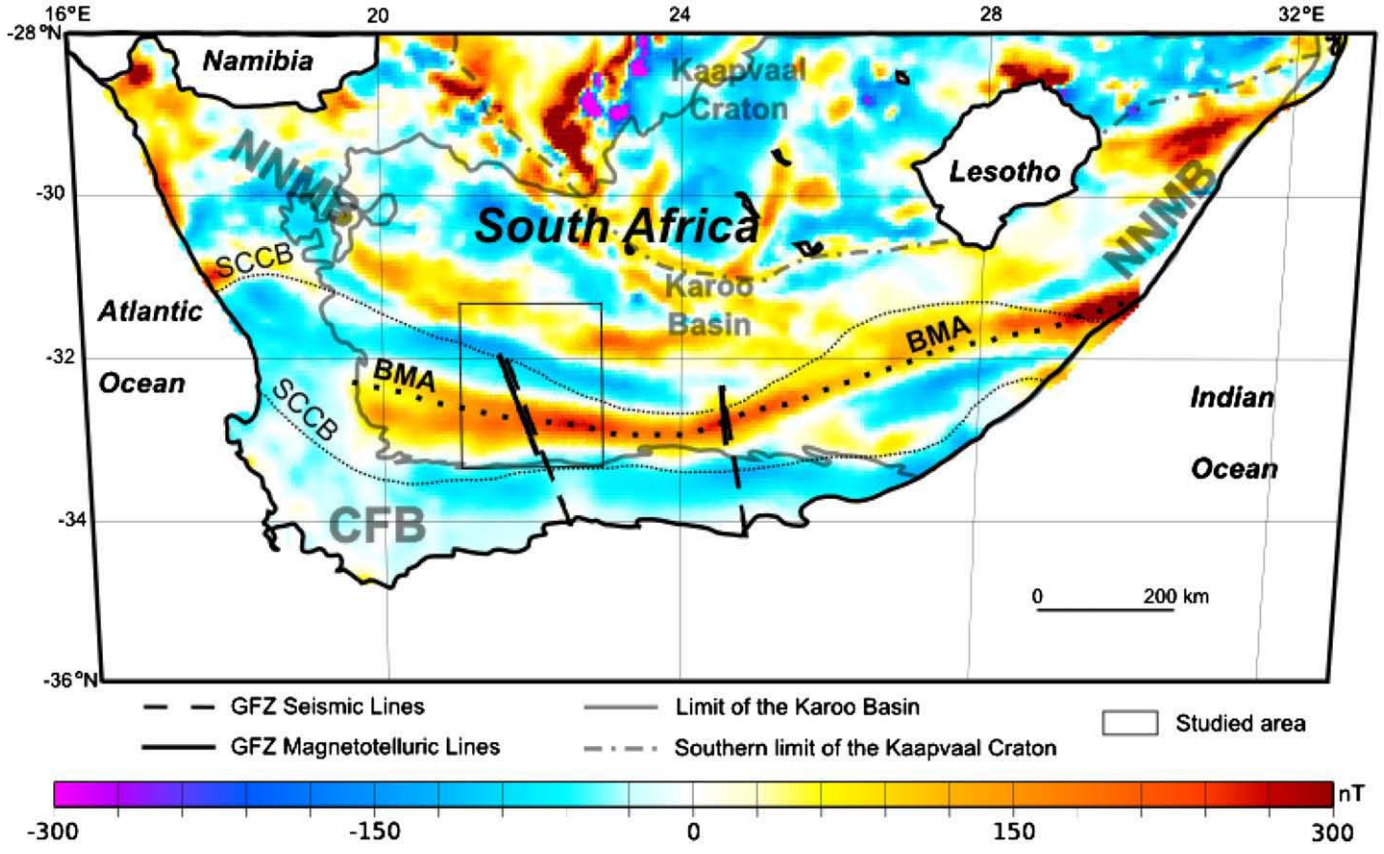

Fig. 1. Magnetic anomaly map at 5 km of altitude over South Africa. Abbreviations: BMA—Beattie Magnetic Anomaly; SCCB—Southern Cape Conductive Belt; NNMB—Namaqua–Natal Mobile Belt; CFB—Cape Fold Belt; GFZ—GeoForschungsZentrum/German Research Center for Geosciences, Potsdam.

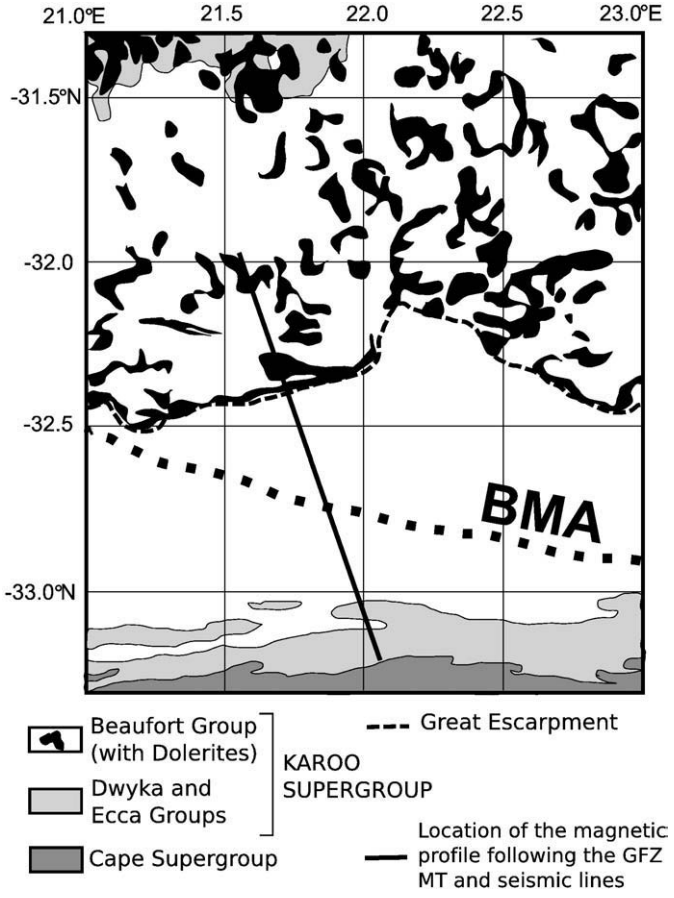

Fig. 2. Simplified geological map of the study area, adapted from Vorster (2003). See Fig. 1 for abbreviations.

Groenewald, 1991; Golynsky and Aleshkova, 2000; Ghidella et al., 2002; Jokat et al., 2003; Ferraccioli et al., 2005). The BMA is not clearly visible on lithospheric models derived from satellite data (Sabaka et al., 2004; Maus et al., 2006; Lesur et al., 2008) suggesting that the root of the BMA source may not be so deep.

Our study focuses on the western part of the BMA, where it starts to split into two branches (Fig. 3). A 145 km long NNW–SSE oriented profile with 68 points every 2.2 km is extracted from the *SANABOZI.txt* dataset in this area, corresponding with the western MT and the seismic reflection profiles (Lindeque et al., 2007; Weckmann et al., 2007a,b) and a part of the western seismic refraction line (Stankiewicz et al., 2007). The BMA along this profile is a wide positive anomaly with two central peaks of 260 nT and two negative edges of about −50 nT (Fig. 4). The central kink shows a decrease of about 50 nT in amplitude. This shape may suggest either the existence of a broad, deep, magnetized body, perhaps accompanied with a thin, shallow, weakly magnetized one, or the interaction of two adjacent magnetized bodies. We test these hypotheses by modeling this profile using one or two magnetic sources.

4. Modeling method

Several methods are available to investigate the source of magnetic anomalies (e.g. Telford et al., 1976; Blakely, 1995). Estimating the width, the depth and the magnetization associated with the source of the BMA is possible using one or two similar bodies with simple shape. In our study, uniformly magnetized spheres (equivalent to dipoles; Blakely, 1995), rectangular prisms (Talwani, 1965; Plouff, 1976) and horizontal cylinders (Parker Gay, 1965; Blakely, 1995) are considered. By a forward approach (*i.e.* by trial-and-error and/or discrete systematic research), the parameters of these objects are adjusted to predict the observations. The quality of the model is evaluated by the parameter *Fit* expressed as:

$$\text{Fit} = 100^{*}\left(1-\sqrt{\frac{\sum_i \left(B_i^o - B_i^c\right)^2}{\sum_i {B_i^o}^2}}\right)$$

where B_i^o and B_i^c are the observed and calculated magnetic anomaly values, respectively.

For the sphere cases, an additional inversion step is performed to refine the model. The equations of the magnetic field anomaly generated by a dipole are used (Blakely, 1995). Six parameters (the three components of the moment and location vectors) then characterize the source. A generalized non-linear scheme with least-square criterion is used (Tarantola and Valette, 1982). The inversion starts with an *a priori* dipole model corresponding to the sphere forward model, and ends either when the chi-squared criterion approaches 1, or when the parameters do not change significantly between two successive iterations. The gaussian distribution (around 0) of the residuals is *a posteriori* checked.

A similar approach was developed by McGrath and Hood (1973), and applied by Frawley and Taylor (2004) andQuesnel et al. (2007) to study the Martian magnetic field anomalies. Further details are indicated in Quesnel (2006),Quesnel et al. (2007, 2008). Although several anomalies can be investigated in a single run using a regional aeromagnetic dataset (Quesnel, 2006; Quesnel et al., 2007), in the present case only one NNW–SSE profile is studied because of the E–W elongation of the BMA.

In order to predict the total-field magnetic anomaly, the main magnetic field strength and orientation at the data acquisition epoch are needed. Here the 10th International Geomagnetic Reference Field (IGRF) model is used for year 1980 (Macmillan and Maus, 2005). Over the study area, it indicates a geomagnetic field intensity of about 28500 nT, an inclination of −66°, and a declination of −22° in 1980.

5. Modeling results

In this section, we present our simple magnetic modeling results along a profile across the BMA, using one or two magnetized bodies.

5.1. One body case

The parameters of the best-fitting models are shown in Table 1, and the predictions are compared with the observations in Fig. 4.

Whatever single body was introduced, the parameter *Fit* was always below 80%, showing that one isolated homogeneously magnetized object with a simple shape may not be the source of the BMA in our study area. The inversion slightly improves the quality of the sphere model, although only light constraints were applied to the dipole parameters. Fig. 4 indicates that only the thin sheet-like prism can create an anomaly with a central kink, but it does not fit the exact shape of the observed kink. This body is located between a 9 and 14-km depth range, *i.e.* in the middle crust (Lindeque et al., 2007), whereas the other model bodies are too deep, probably below the Curie depth and the Moho in this area (about 42 km according to Harvey et al., 2001; Nguuri et al., 2001; Stankiewicz et al., 2002). The wavelength of the observed anomaly is too large to be explained by one dipole or line of dipoles shallower than 50 km. This is not surprising because the dipoles concentrate the magnetization in one point. The magnetization intensities are large, even for the shallow prism (6 A m^{-1}), but the inclination and declination differ of more than 40° from the induced field directions in this region.

We conclude that, if one object is used to predict the BMA along this profile, then it may correspond to a 60 km wide magnetized layer located in the middle crust.

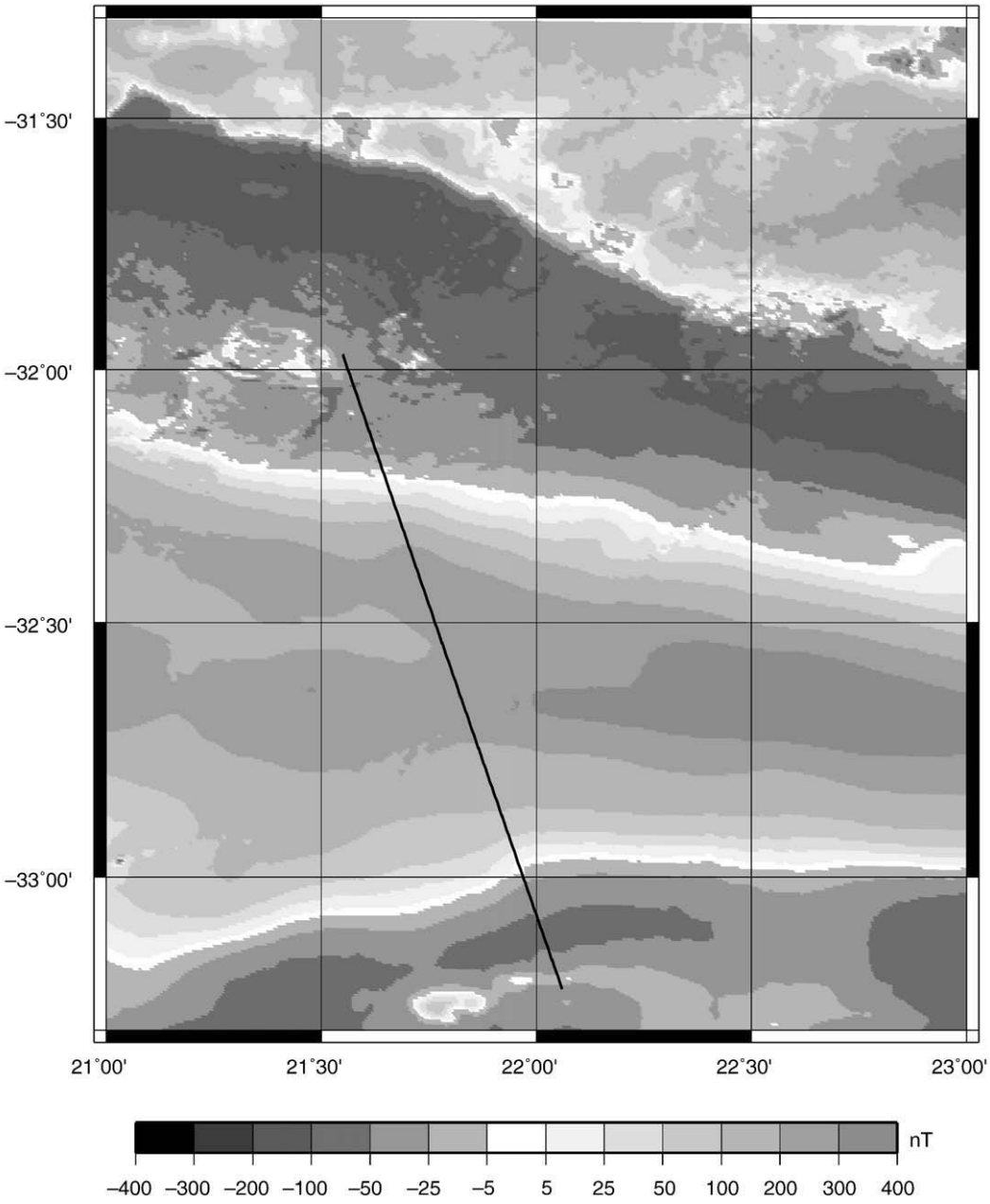

Fig. 3. Magnetic anomaly map at 1 km of altitude over the study area. The solid line shows the location of the selected magnetic profile, following the MT and seismic lines indicated in Figs. 1 and 2.

5.2. Two body case

Table 2 presents the best parameters of each two-body forward model, whereas Table 3 shows the parameters of the two dipoles resulted from the inversion of the magnetic data along this profile. The associated predicted anomalies are compared to the observed one in Fig. 5.

The parameter *Fit* is always above 85%. The correlation coefficient reaches 0.99 for all models. This indicates that two magnetized sources are more likely to explain the BMA than one single source. The inversion allows to refine the sphere model, increasing the parameter *Fit* by 2%. As for the one-body case, the depths of spheres, dipoles and cylinders are below 25 km, corresponding to the lower crust top (Lindeque et al., 2007), but they do not exceed the Curie depth and the Moho (Harvey et al., 2001; Nguuri et al., 2001; Stankiewicz et al., 2002). The best two-body model correspond to the thin two-prism case (Fit ~ 88%). These prisms are located between 9 and 18 km in the middle crust (Lindeque et al., 2007). Their magnetization intensities of 5 and 6 A m^{-1} are similar to the single prism model. Taking the length of the two prisms into account, the total N–S extent of the magnetized object is about 80 km. The improvement in comparison to the single prism model is due to the vertical offset between the two prisms at −32.65°N, which leads to a better prediction of the central kink of the BMA. For the dipolar bodies, predictions also show a central kink. The resulting models indicate a more distinct offset with a northern object shallower than the southern object. This may suggest a southward dip of a single magnetized source. However, the magnetization parameters can also differ between two adjacent sources (*e.g.* for the sphere and cylinder cases), reducing the plausibility of this assumption. An alternate model would be a vertical contrast of magnetization (*e.g.* due to a fault or shear zone).

The average of the inclination values is about −62°, whereas it is about −21° for the one-body models. For declination values, the averages are −28° and 81° for the two- and one-body models, respectively. Thus

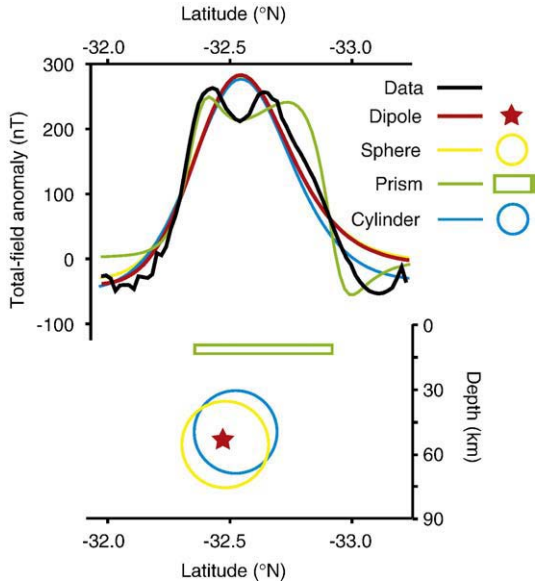

Fig. 4. Results of the modeling of the BMA along the selected profile, using a single source.

the remanent magnetization of the two-body models seems less important than for the one-body model. The declinations of the two cylinders are equal to −123°, *i.e.* 100° different from the induced field declination ($D=-22°$), but this difference is attenuated by the large inclinations (−65°) close to the induced field inclination ($I=-66°$). A cylinder with similar magnetization parameters corresponds to the best model to predict the BMA toward the East, where its amplitude is maximum (results not shown). It suggests that the horizontal cylinder with infinite lateral extent is a good analogue to represent an elongated magnetized source. However, along the selected profile, two magnetized prisms are more likely to predict the BMA. Moreover, the top of the prism, commonly interpreted as the top of the magnetized source, is 9 km in the present case. This depth also corresponds to the maximum depth for which downward continuation of the BMA measurements is stable.

6. Discussion

The previous section described our magnetic modeling results along a profile across the BMA. This profile follows the western MT and seismic lines (Figs. 1–3). In the following, we compare our results with the models derived from both independent geophysical experiments. Then, we discuss the implications on the nature of the source of the BMA.

6.1. Comparison with other geophysical data

In Fig. 6, the two uniformly magnetized prisms that predict 88% of the BMA profile are plotted over the western MT and seismic refraction cross-sections (Stankiewicz et al., 2007; Weckmann et al., 2007a,b). Since the seismic refraction image of the upper and middle crust (Stankiewicz et al., 2007) is almost equivalent to the seismic reflection image in this area (Lindeque et al., 2007), we only compare our magnetic modeling results with the former. The MT electrical conductivity section corresponds to the Fig. 7 of Weckmann et al. (2007a), whereas the seismic image is taken from the Fig. 4a of Stankiewicz et al. (2007).

6.1.1. Comparison with the MT model

The MT experiment provides a high-resolution image of the crustal electrical conductivity along this profile (Weckmann et al., 2007a,b). Shallow and small-scale conductivity structures cannot be compared with our simple magnetization model, whereas large-scale conductivity anomalies are more suitable for comparison. Based on the assumption that the BMA and the SCCB have a common source (see section 2), we would expect that the simple magnetic bodies correlate with zones of high conductivity (red colors in the middle panel of Fig. 6). In fact, a very prominent high conductivity anomaly is located in upper- to mid-crustal levels at about 100 km of distance along the profile. Conductive (<20 Ω m) zones still might be present at depths corresponding to the center of the southern prism, but highly resistive zones also correlate very well its lateral edges. Farther to the north, high conductive synform structures are observed. Again, the edges of the northern sheet-like magnetic body seems to outline resistive zones, but it is less clear than for the southern prism because it crosses the conductive synforms.

6.1.2. Comparison with the seismic model

Stankiewicz et al. (2007) identified a high-velocity zone (up to 7 km^{-1} P-wave velocity) just beneath the axis of the BMA, between 10 and 20 km in the crust (Fig. 6). The location of our northern sheet-like magnetic body fits the location of this high-velocity zone (Fig. 6), suggesting a common geological source. Lindeque et al. (2007) also associated this high-velocity zone to a 10 km wide and 7 to 15 km deep zone of high seismic reflectivity that may be related to the source of the BMA. If the two magnetic bodies belong to the same magnetic source, then it would need to be either southward-dipping or offset by a fault. However, no such fault was detected by the reflection study of Lindeque et al. (2007), and these authors also concluded the tectonic fabric dips north at the corresponding depth. Furthermore, if the two sheet-like magnetic bodies were part of the same body, then a corresponding high-velocity zone should be expected to mark the

Table 1
Parameters of the magnetized sphere, prism, cylinder and dipole assuming a single source to explain the BMA in the studied area.

Parameters	Sphere	Prism	Cylinder	Dipole
Latitude (°N)	−32.48	−32.93/−32.37	−32.52	−32.47 (0.02)
Longitude (°E)	21.80	21.60/22.00	21.80	21.80 (0.01)
Depth (km)	55	9/14	50	53.6 (0.9)
Radius (km)	22	–	20	–
Magnetization (A m^{-1})	14	6	10	–
Dipolar moment (A m^2)	6.24×10^{14}	7.03×10^{13}	–	$6.55\ (0.97)\times10^{14}$
Inclination (°)	−23	−22	−17	−22.5 (0.1)
Declination (°)	92	60	80	92.6 (0.1)
Fit (%)	74.3	78.2	76.4	74.5

For the sphere and prism cases, dipolar moments correspond to the product of the magnetization with the volume. This parameter cannot be determined for the horizontally infinite cylinder (equivalent to a line of dipoles). The parameters of the dipole differ from those of the sphere forward model because they result from inversion of the magnetic data using a minimum standard deviation set to 28 nT. Associated standard deviations for the parameters are shown in parentheses.

Table 2
Parameters resulting from forward modeling assuming two adjacent sources with similar shape to explain the BMA.

Parameters	Spheres		Prisms		Cylinders	
Latitude (°N)	−32.40	−32.80	−32.65/−32.33	−33.65/−32.05	−32.40	−32.72
Longitude (°E)	21.7	21.8	21.6/21.8	21.6/21.9	21.8	21.8
Depth (km)	33	36	9/12	13/18	20	40
Radius (km)	11	11	–	–	5	14
Magnetization (A m^{-1})	7	13	5	6	7	5
Inclination (°)	−45	−64	−84	−75	−65	−65
Declination (°)	180	−60	−150	0	−123	−133
Fit (%)	85.3		87.9		87.0	

Table 3
Parameters of the dipoles resulting from inversion of the magnetic measurements along the selected profile.

Parameters	Northern dipole	Southern dipole
Latitude (°N)	−32.4 (0.1)	−32.8 (0.1)
Longitude (°E)	21.7 (0.1)	21.8 (0.1)
Depth (km)	28.6 (2.8)	38.2 (3.5)
Dipolar moment (A m^2)	4.0 (0.9)×10^{13}	9.0 (0.1)×10^{13}
Inclination (°)	−31.0 (0.2)	−64.4 (0.1)
Declination (°)	128.8 (0.9)	−76.7 (1.1)
Fit (%)	87.3	

Minimum standard deviation of the data is equal to 28 nT. Parameter standard deviations are shown in parentheses.

southern prism as well. In contrast, the southern prism coincides with velocities in the region of 6 km^{-1}. Therefore, seismic images argue against the hypothesis that the two prisms represent the same body, but they support a source at mid- to lower-crustal depths.

6.2. Sources of the BMA

Based on the new results from MT and seismic experiments, alternative interpretations of the possible geological origin of the BMA have to be discussed. Despite the simple shapes assigned to our magnetized models, some correlations have been noted with the geophysical images provided by the recent MT and seismic surveys. The best-fitting (two prisms) model argues in favor of highly-magnetized zones in the middle crust, whereas the two-dipole or line of dipole models indicate magnetized source depths reaching lower crustal levels. A broad magnetic source that extends to the lower crust was also suggested by Weckmann et al. (2007b), who used 2.5D magnetic forward modeling module, based on the Rasmussen and Pedersen (1979) method, within the WinGLink software package (http://www.geo-system.net).

The discussion on a possible broad source for the BMA has been strongly tied to the existence and interpretation of the SCCB (e.g. de Beer et al., 1982; Pitts et al., 1992). The SCCB was inferred from measurements using an array of 24 three-component magnetometers with an average site spacing in the order of hundred kilometers (Gough, 1973). High-resolution MT measurements across the SCCB however suggest that the SCCB is not a deep and broad homogeneous zone of high conductivity, but is the integration of a series of localized zones of high conductivities within the Namaqua–Natal Mobile Belt basement (Weckmann et al., 2007a,b).

Based on this apparent spatial correlation of the BMA and the SCCB in the 80s, a common source in the form of a 50 km wide southward dipping sliver of serpentinized palaeo-oceanic crust that reached to depths of 30 km was suggested to be the cause of both these anomalies (e.g. de Beer et al., 1982; Pitts et al., 1992; Harvey et al., 2001). The high magnetization intensity predicted by our preferred model could correspond to serpentinites, because similar values were observed for serpentinites belonging to a palaeo-oceanic suture in the Alps (Shive et al., 1988; Shive, 1990). Such rocks also show seismic velocities comparable to those estimated for the high-velocity zone beneath the BMA (about 7 *km s*$^{-1}$; see Horen et al., 1996). They could lastly be associated with zones of high electrical conductivity, but only in active regimes (with fluids). Modern electrical conductivity measurements on serpentinite without fluids reveal it as a poor electrical conductor (Airo and Loukola-Ruskeeniemi, 2004). It would become electrically conductive if the magnetite is interconnected over a large area. These interconnection can occur through shearing processes along a fault zone and may be a possible explanation for the localized mid-crustal high conductivity zone at 100 km of distance along the profile of this study (Fig. 6). For instance, results from MT experiments in a similar tectonic setting in the Damara Belt in Namibia suggest that fossil shear zones become visible with MT in presence of graphite or other mineralizations on shear planes (Weckmann et al., 2003; Ritter et al., 2003). A more detailed discussion on possible conductivity mechanisms in active and fossil regimes can be found in Ritter et al. (2005). Additionally, our model indicates that the BMA source magnetization is less remanent than typically expected for serpentinized rocks (Shive et al., 1988; Shive, 1990; Florio et al., 1994). Other studies also showed that serpentinites in suture zones may not possess such high magnetization values due to a generally low serpentinization degree (Saad, 1969; Lienert and Wasilewski, 1979).

Magnetite in serpentinite is not the only possible mineral to carry large and deep magnetization in the Earth's crust. Nanoscale exsolution intergrowth of titanohematite and ilmenite has been proven to cause large crustal geomagnetic anomalies (McEnroe et al., 2001, 2002). Such mineralizations are also observed in gneisses and granulites (Williams et al., 1985; Robinson et al., 2002). These rocks cool slowly at depth ranges equivalent to what our modeling results suggest. Furthermore, the seismic velocities observed are also in agreement with those of granulite-facies rocks (Kanao and Ishikawa, 2004). However, the remanent component of our modeled magnetization should be more significant to be consistent with the large amount of natural remanent magnetizations typical for granulite rocks (McEnroe et al., 2001). On the other hand, the presence of a fault zone might diminish or perturbate the remanent component of its magnetization. The two-body magnetized models show a vertical offset which may represent such tectonic feature. However, its position is different from what Weckmann et al. (2007b) interpreted as a shear zone cutting through a broad magnetic body, and the seismic reflection image does not show such fault (Lindeque et al., 2007).

7. Conclusions

In this study, uniformly magnetized spheres, prisms and cylinders are used to represent as simply as possible the source of the continental-scale BMA in South Africa along a single aeromagnetic profile, which follows recent MT and seismic lines. The parameters of these objects are adjusted by forward modeling and inversion. Our results suggest that two similar sources with a vertical offset are more likely than a single source in order to explain the shape of the BMA in this region. The best-fitting model corresponds to two wide (~80 km) and highly-magnetized (more than 5 A m^{-1}) sheet-like prisms which

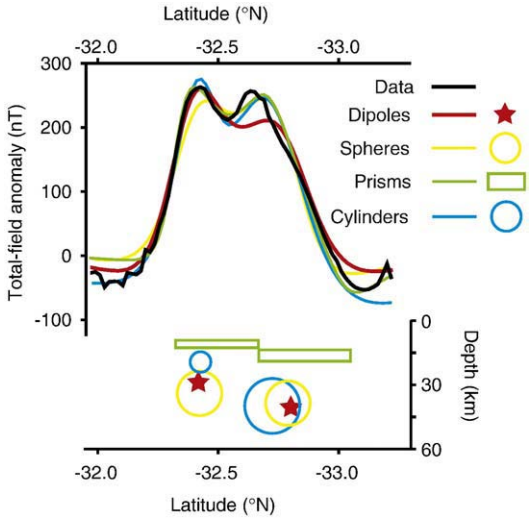

Fig. 5. Results of the modeling of the BMA along selected profile, using two sources.

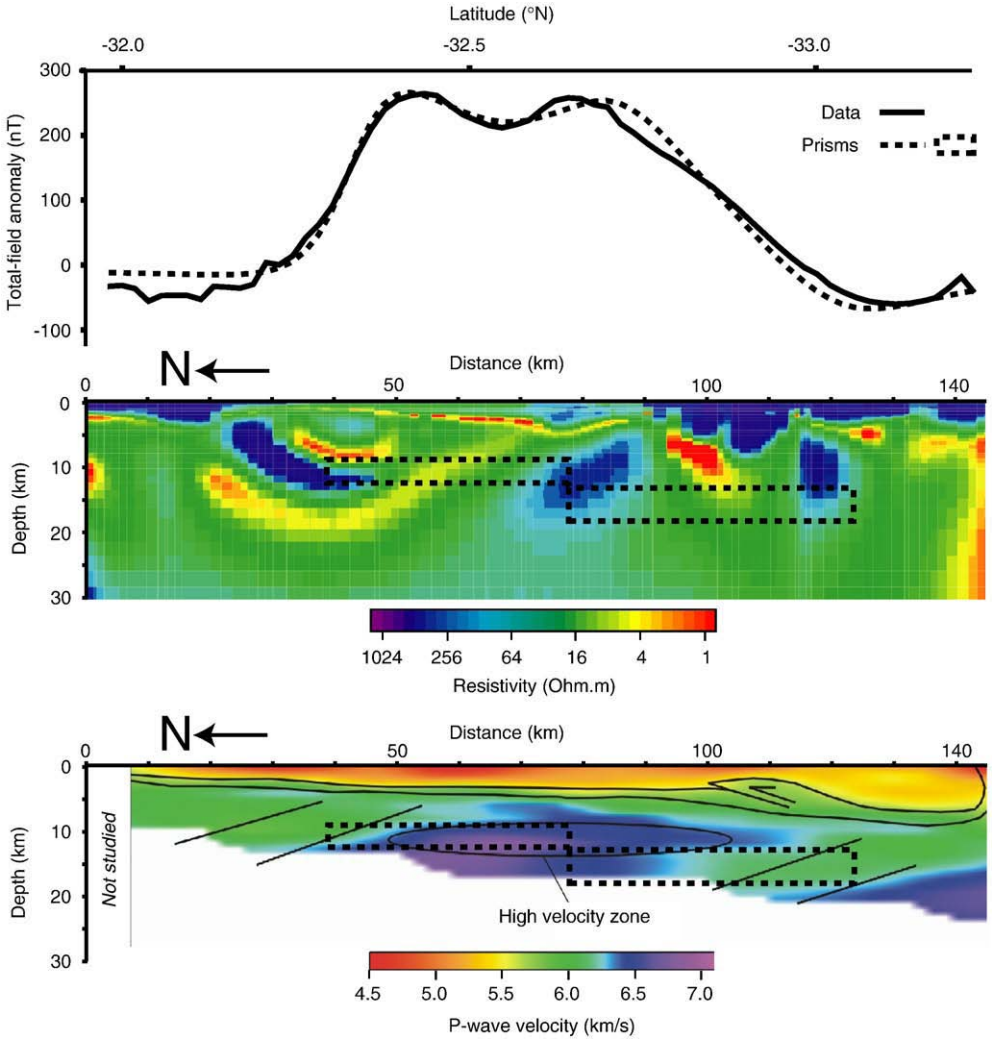

Fig. 6. Comparison of the resulting magnetic prisms (dashed line) with the interpretation of western MT (central panel) and seismic refraction (bottom panel) lines. Note that the seismic refraction experiment starts 7 km southward than the MT profile. The top panel compares the observed total-field anomaly with the anomaly predicted by the two prisms (same as in Fig. 5). The southern prisms seem to outline the resistive zones in the middle crust, whereas a clear similar correlation for the northern prism is difficult. The location of the northern prism on the other hand matches a high-velocity zone in the seismic tomography image. However, the southern prism (with similar magnetization than the northern one) correlates with a low-velocity zone.

are located at mid-crustal depths (~10–20 km). Other, less-preferred models show that thicker bodies with enhanced crustal magnetization might extend into the lower crust. The mean magnetization direction of the two-body models are dominated by the induced field direction, even if a weak remanence appears to be needed to fit the exact shape of the BMA. We find some correlations with the interpretation of MT and seismic results in the same region. The edges of the southern prism of our best-fitting model seem to outline a zone of low electrical conductivities in the middle crust. The location of the northern prism seems to correlate with a zone of high-velocity which may represent the source of the BMA. However, the southern prism (with similar magnetization than the northern one) correlates with a low-velocity zone, and the northern prism does not show a clear correlation with resistive structures of the MT model. The rather weak remanent magnetization component of the magnetized prisms may argue against the previously suggested presence of serpentinized palaeo-oceanic crust as the source of the BMA. As an alternative source, we suggest a wide highly-magnetized body, possibly related to granulite-facies rocks with exsolved hematite–ilmenite. In our study area, this magnetic body appears to be cut by a shear zone or a fault, but the MT and seismic results do not support this hypothesis. Therefore, further geophysical and geological investigations are needed.

Acknowledgments

We would like to thank M. Hamoudi for a helpful discussion and the information about the dataset. We also thank M. de Wit and the SADC for the original aeromagnetic dataset of South Africa. We thank F. Ferracioli for his comments and suggestions, and an anonymous referee. YQ and UW were supported by the German Science Foundation DFG. We thank the Geophysical Instrument Pool Potsdam for providing the MT and the seismic equipments. This is Inkaba yeAfrica contribution 30.

References

Airo, M., Loukola-Ruskeeniemi, K., 2004. Characterization of sulfide deposits by airborne magnetic and gamma-ray responses in eastern Finland. Ore Geol. Rev. 24, 67–84.
Blakely, R., 1995. Potential Theory in Gravity and Magnetic Applications. Cambridge University Press, Cambridge.
Cloetingh, S., Lankreijer, A., de Wit, M., Martinez, H., 1992. Subsidence history analysis and forward modeling of the Cape and Karoo Supergroups. In: de Wit, M., Ransome, I. (Eds.), Inversion Tectonics of the Cape Fold Belt, Karoo and Cretaceous Basins of Southern Africa. A. A. Balkema, Brookfield, Vt., pp. 239–249.
Corner, B., 1989. The Beattie anomaly and its significance for crustal evolution within the Gondwana framework. First Technical Meeting of the S. Afr. Geophys. Assoc., Johannesburg, pp. 15–17.

Corner, B., Groenewald, P., 1991. Gondwana reunited. S. Afr. Trans. Nav. Antarkt. 21 (2), 172.
de Beer, J., van Zijl, J., Gough, D., 1982. The Southern Cape Conductive Belt (South Africa): its composition, origin and tectonic significance. Tectonophysics 83, 205–225.
de Wit, M., Ransome, I., 1992. Inversion Tectonics of the Cape Fold Belt, Karoo and Cretaceous Basins of Southern Africa. Balkema, Rotterdam.
Ferraccioli, F., Jones, P., Curtis, M., Leat, P., Riley, T., 2005. Tectonic and magmatic patterns in the Jutulstraumen rift (?) region, East Antarctica, as imaged by high-resolution aeromagnetic data. Earth Planets Space 57, 767–780.
Florio, G., Rapolla, A., Fedi, M., Fountain, D.M., Shive, P.N., 1994. Reply to "Comments on anisotropic magnetic susceptibility in the continental lower crust and Its implications for the shape of magnetic anomalies" by P. Rochette. Geophys. Res. Lett. 21 (24), 2775–2776.
Frawley, J., Taylor, P., 2004. Paleo-pole positions from martian magnetic anomaly data. Icarus 172 (2), 316–327.
Ghidella, M., Yanez, G., LaBrecque, J., 2002. Revised tectonic implications for the magnetic anomalies of the Western Weddell Sea. Tectonophysics 347, 65–86.
Golynsky, A., Aleshkova, N., 2000. Regional magnetic anomalies of the Weddell Sea region and their geological significance. Polarforschung 67 (3), 101–117.
Gough, D., 1973. The geophysical significance of geomagnetic variation anomalies. Phys. Earth Planet. Int. 7 (3), 379–388.
Harvey, J., de Wit, M., Stankiewicz, J., Doucoure, C., 2001. Structural variations of the crust in the southwest Cape, deduced from seismic receiver functions. S. Afr. J. Geol. 104, 231–242.
Horen, H., Zamora, M., Dubuisson, G., 1996. Seismic wave velocities and anisotropy in serpentinized peridotites from Xigaze ophiolite: abundance of serpentine in slow spreading ridge. Geophys. Res. Lett. 23 (1), 9–12.
Jokat, W., Boebel, T., König, M., Meyer, U., 2003. Timing and geometry of early Gondwana breakup. J. Geophys. Res. 108 (B9), 2428. doi:10.1029/2002JB001802.
Kanao, M., Ishikawa, M., 2004. Origins of the lower crustal reflectivity in the Lützow–Holm Complex, Enderby Land, East Antarctica. Earth Planets Space 56, 151–162.
Korhonen, J., Fairhead, J., Hamoudi, M., Hemant, K., Lesur, V., Mandea, M., Maus, S., Purucker, M., Ravat, D., Sazonova, T., Thébault, E., 2007. Magnetic Anomaly Map of the World, Scale 1:50,000,000, 1st Edition. Commission for the Geological Map of the World, UNESCO Edition.
Lesur, V., Wardinski, I., Rother, M., Mandea, M., 2008. GRIMM—The GFZ Reference Internal Magnetic Model based on vector satellite and observatory data. Geophys. J. Int. 173, 382–394.
Lienert, B., Wasilewski, P., 1979. A magnetic study of the serpentinization process at Burro Mountain, California. Earth Planet. Sci. Lett. 43, 406–416.
Lindeque, A., Ryberg, T., Stankiewicz, J., Weber, M., de Wit, M., 2007. Deep crustal seismic reflection experiment across the southern Karoo Basin, South Africa. S. Afr. J. Geol. 110, 419–438.
Macmillan, S., Maus, S., 2005. International geomagnetic reference field—the tenth generation. Earth Planets Space 57, 1135–1140.
Maus, S., Rother, M., Hemant, K., Stolle, C., Lühr, H., Kuvshinov, A., Olsen, N., 2006. Earth's lithospheric magnetic field determined to spherical harmonic degree 90 from CHAMP satellite measurements. Geophys. J. Int. 164, 319–330. doi:10.1111/j.1365-246X.2005.02833.x.
McEnroe, S., Harrison, R., Robinson, P., Golla, U., Jercinovic, M., 2001. Effect of fine-scale microstructures in titanohematite on the acquisition and stability of natural remanent magnetization in granulite facies metamorphic rocks, southwest Sweden: implications for crustal magnetism. J. Geophys. Res. 106 (B12), 30523–30546.
McEnroe, S., Harrison, R., Robinson, P., Langenhorst, F., 2002. Nanoscale haematite–ilmenite lamellae in massive ilmenite rock: an example of 'lamellar magnetism' with implications for planetary magnetic anomalies. Geophys. J. Int. 151, 890–912.
McGrath, P., Hood, P., 1973. An automatic least-squares multimodel method for magnetic interpretation. Geophysics 38 (2), 349–358.
Nguuri, T., Gore, J., James, D., Webb, S., Wright, C., Zengeni, T., Gwavava, O., Snoke, J., 2001. Crustal structure beneath southern Africa and its implications for the formation and evolution of the Kaapvaal and Zimbabwe cratons. Geophys. Res. Lett. 28, 2501–2504.
Parker Gay, S., 1965. Standard curves for magnetic anomalies over long horizontal cylinders. Geophysics 30 (5), 818–828.
Pitts, B., Mahler, M., de Beer, J., Gough, D., 1992. Interpretation of magnetic, gravity and magnetotelluric data across the Cape Fold Belt and Karoo Basin. In: de Wit, M., Ransome, I. (Eds.), Inversion Tectonics of the Cape Fold Belt, Karoo and Cretaceous Basins of Southern Africa. A. A. Balkema, Brookfield, Vt., pp. 27–32.
Plouff, D., 1976. Gravity and magnetic fields of polygonal prisms and application to magnetic terrain corrections. Geophysics 41 (4), 727–741.
Quesnel, Y., 2006. Interprétation des données magnétiques martiennes: contraintes sur l'évolution primitive de Mars. Ph.D. thesis, Université de Nantes, available at: http://www.bu.univ-nantes.fr/sciences/docnum/2006/quesnel_yoann.pdf. (in French).
Quesnel, Y., Langlais, B., Sotin, C., 2007. Local inversion of magnetic anomalies: implication for Mars' crustal evolution. Planet. Space Sci. 55 (3), 258–269.
Quesnel, Y., Langlais, B., Sotin, C., Galdéano, A., 2008. Modeling and inversion of local magnetic anomalies. J. Geophys. Eng. 5, 387–400.
Rasmussen, R., Pedersen, L., 1979. End corrections in potential field modelling. Geophys. Prospect. 749–760.
Ritter, O., Weckmann, U., Vietor, T., Haak, V., 2003. A magnetotelluric study of the Damara Belt in Namibia 1. Regional scale conductivity models. Phys. Earth Planet. Int. 138, 71–90. doi:10.1016/S0031-9201(03)00,078-5.
Ritter, O., Hoffmann-Rothe, A., Bedrosian, P., Weckmann, U., Haak, V., 2005. Electrical conductivity images of active and fossil fault zones. In: Bruhn, D., Burlini, L. (Eds.), High-Strain Zones: Structure and Physical Properties, vol. 245. Geological Society of London Special Publications, pp. 165–186.
Robinson, P., Harrison, R., McEnroe, S., Hargraves, R., 2002. Lamellar magnetism in the haematite–ilmenite series as an explanation for strong remanent magnetization. Nature 418, 517–520.
Saad, A., Dec. 1969. Magnetic properties of ultramafic rocks from Red Mountain, California. Geophysics 34 (6), 974–987.
Sabaka, T., Olsen, N., Purucker, M., 2004. Extending comprehensive models of the Earth's magnetic field with Orsted and CHAMP data. Geophys. J. Int. 159, 521–547.
Shive, P., 1990. The Ivrea Zone and lower crustal magnetization. Tectonophysics 182, 161–167.
Shive, P., Frost, B., Peretti, A., 1988. The magnetic properties of metaperidotitic rocks as a function of metamorphic grade: implications for crustal magnetic anomalies. J. Geophys. Res. 93, 12187–12195.
South African Committee on Stratigraphy, 1980. Stratigraphy of South Africa, Handbook 8. Tech. rep., Geological Survey of South Africa.
Stankiewicz, J., Chevrot, S., van der Hilst, R., de Wit, M., 2002. Crustal thickness, discontinuity depth, and upper mantle structure beneath southern Africa: constraints from body wave conversions. Phys. Earth Planet. Int. 130, 235–251.
Stankiewicz, J., Ryberg, T., Schulze, A., Lindeque, A., Weber, M., de Wit, M., 2007. Initial results from wide-angle seismic refraction lines in the Southern Cape. S. Afr. J. Geol. 110, 407–418.
Talwani, M., 1965. Computation with the help of a digital computer of magnetic anomalies caused by bodies of arbitrary shape. Geophysics 30, 797–817.
Tarantola, A., Valette, B., 1982. Generalized nonlinear inverse problems solved using the least squares criterion. Rev. Geophys. Space Phys. 20, 219–232.
Telford, W., Geldart, L.P., Sheriff, R., Keys, D., 1976. Applied Geophysics. Cambridge University Press, Cambridge. 1988 version.
Thomas, R., Marshal, C., du Plessis, A., Fitch, F., Miller, J., von Brunn, V., Watkeys, M., 1992. Geological studies in southern Natal and Transkei: implications for the Cape Orogen. In: de Wit, M., Ransome, I. (Eds.), Inversion Tectonics of the Cape Fold Belt, Karoo and Cretaceous Basins of Southern Africa. A. A. Balkema, Brookfield, Vt., pp. 229–236.
Vorster, C., 2003. Simplified geology of South Africa, Lesotho and Swaziland. South African Council for Geoscience Edition.
Weckmann, U., Ritter, O., Haak, V., 2003. A magnetotelluric study of the Damara Belt in Namibia 2. Internal structure of the Waterberg Fault/Omaruru Lineament. Phys. Earth Planet. Int. 138, 91–113. doi:10.1016/S0031-9201(03)00,079-7.
Weckmann, U., Ritter, O., Jung, A., Branch, T., de Wit, M., 2007a. Magnetotelluric measurements across the Beattie magnetic anomaly and the Southern Cape Conductive Belt, South Africa. J. Geophys. Res. 112 (B11). doi:10.1029/2005JB0039755.
Weckmann, U., Jung, A., Branch, T., Ritter, O., 2007b. Comparison of electrical conductivity structures and 2D magnetic modelling along two profiles crossing the Beattie Magnetic Anomaly, South Africa. S. Afr. J. Geol. 110, 449–464.
Williams, M., Shive, P., Fountain, D., Frost, B., 1985. Magnetic properties of exposed deep crustal rocks from the Superior Province of Manitoba. Earth Planet. Sci. Lett. 76, 176–184.